Shape-Dominated Ordering in Nematic Solvents. A Deuterium NMR Study of Cycloalkane Solutes

Andreas F. Terzis,[†] Chi-Duen Poon,[†] Edward T. Samulski,*[,†] Zeev Luz,[‡] Raphy Poupko,[‡] Herbert Zimmermann,[‡] Klaus Müller,[‡] Hirokazu Toriumi,[§] and Demetri J. Photinos[⊥]

Contribution from the Department of Chemistry, University of North Carolina, Chapel Hill, North Carolina 27599-3290, Weizmann Institute of Science, Rehovot, Israel 76100, Department of Chemistry, University of Tokyo, Komaba, Tokyo 153, Japan, and Department of Physics, University of Patras, Patras, Greece 26110

Received September 7, 1995[⊗]

Abstract: We examine a series of closely related, relatively inert, cyclic aliphatic solutes—cyclohexane, methylcyclohexane, 1,1-dimethylcyclohexane, 1,4-*trans*-dimethylcyclohexane, 1,4-*cis*-dimethylcyclohexane, *trans*-decalin, and *cis*-decalin—in a nematic solvent and demonstrate that their orientational ordering can be accurately described in terms of purely hard-body interactions with the solvent molecules. These interactions are treated explicitly in the context of a statistical mechanical approximation wherein the orientational correlations among the solvent molecules are not taken into account directly. We test the theory by predicting the observed order parameters of the aliphatic solutes as determined with deuterium nuclear magnetic resonance. The utility and limitations of a description of solute ordering derived exclusively from hard-body interactions is discussed.

I. Introduction

It is well known that the intermolecular structure and the diffusive motions in simple liquids are determined primarily by short-ranged, repulsive intermolecular forces[1] and that the same is true for liquid crystals.[2−6] Furthermore, these forces in their hard-body idealization, starting with the pioneering work of Onsager,[7] have been shown to be sufficient for the creation of long-range orientational order in systems of anisometric molecules, a prediction that has been verified and amplified by more recent computer simulations of hard-body molecules.[5,6] In fact, such simulations show that all the common liquid crystalline phases can be obtained at high densities as a result of packing restrictions on molecules with anisotropic shapes. This, of course, is not to imply that in real liquid crystals the various types of longer-ranged forces are totally irrelevant. To the contrary, first there is the Maier−Saupe[8] theory which is the antithesis of the Onsager view: The Maier−Saupe theory posits that a nematic phase can result from the attractive forces, associated with the anisotropy of molecular polarizability. Second, particular types of site-specific intermolecular forces, such as electrostatic and hydrogen bonding, in certain cases are known to play a decisive phase stabilizing (or destabilizing) role and also to give rise to various molecular association effects.[9,10] Finally, longer-ranged attractive forces are introduced in order to stabilize liquid-crystalline phases even in cases where the anisotropy is assumed to be produced entirely by the short range repulsions.[2,3]

In a certain sense, the theories put forward by Onsager and by Maier and Saupe had rather modest goals—to show that the nematic-to-isotropic phase transition is sensitive to idealized mesogen attributes (e.g., the mesogen aspect ratio or its polarizability anisotropy). When considering actual liquid crystals on a quantitative level, however, the ultimate goals—determining the force field for a given mesogen and quantitatively reproducing thermodynamic properties—appear to be discouragingly hard to reach: Mesogens are generally complex molecules, exhibiting various types of interactions and internal motions with mesophase stability often appearing to depend very critically on a delicately balanced interplay of such interactions and motions. Moreover, a reasonably complete statistical mechanical treatment is extremely difficult. The following question is then naturally raised: Is there a simple, quantifiable molecular picture embodying the essential features of mesogen interactions that is capable of providing usable quantitative predictions in the context of some well-defined statistical-mechanical approximation? A particularly expedient route to a first answer to this question is to focus on the interactions of mesogens with probe solutes rather than on the direct mesogen−mesogen interaction. In this way it becomes possible, without appreciably perturbing the structure and the ordering of the mesophase, to selectively probe the different components of the interaction of a given mesogen simply by using judiciously chosen solutes.

Recently, Terzis, and Photinos[11] applied these ideas to the study of the ordering of a number of probe solutes in representative selections of nematic solvents. They found that a consistent and fairly accurate description can be achieved by using a rather simple picture of the molecules whereby the interactions merely consist of hard-body repulsions and forces

[†] University of North Carolina.
[‡] Weizmann Institute of Science.
[§] University of Tokyo.
[⊥] University of Patras.
[⊗] Abstract published in *Advance ACS Abstracts,* February 1, 1996.

(1) Chandler, D.; Weeks, J. D.; Andersen, H. C. *Science* **1983**, *220*, 787.
(2) Gelbart, W. M. *J. Phys, Chem.* **1982**, *86*, 4298.
(3) Cotter, M. A. *Phil. Trans. R. Soc. London* **1983**, *A309*, 127.
(4) Vertogen, G. J.; de Jeu, W. H. *Thermotropic Liquid Crystals, Fundamentals;* Springer: Heidelberg, 1989.
(5) Frenkel, D. *Liq. Cryst.* **1989**, *5*, 929.
(6) Vertogen, G. J.; Lekkerkerker, H. N. W. *Rep. Prog. Phys.* **1992**, *55*, 1241.
(7) Onsager, L. *Am. N. Y. Acad. Sci.* **1949**, *51*, 627.
(8) Maier, W.; Saupe, A. *Z. Naturforsch.* **1958**, *A13*, 564; **1959**, *A14*, 1909; **1960**, *A15*, 282.
(9) de Jeu, W. H. *Phil. Trans. R. Soc. London* **1983**, *A309*, 217.
(10) Cladis, P. E. *Phys. Rev. Lett.* **1975**, *35*, 48.
(11) Terzis, A. F.; Photinos, D. J. *Mol. Phys.* **1994**, *83*, 847.

0002-7863/96/1518-2226$12.00/0

Table 1. The Deuterated Compounds Studied in the Present Work

#	Name	Wt%[a]	Symmetry	Structural Formulae
I	cyclohexane	2.3	D_{3d}	
II	methylcyclohexane	2.9	C_S	
III	1,1-dimethylcyclohexane	2.5	C_S	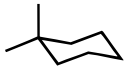
IV	1,4-*cis*-dimethylcyclohexane	3.1	C_S	
V	1,4-*trans*-dimethylcyclohexane	2.9	C_{2h}	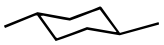
VI	*trans*-decalin	3.0	C_{2h}	
VII	*cis*-decalin	4.2	C_2	

[a] Weight percent of solute in the ZLI2452 solvent used in the experiments.

originating from the permanent electrostatic moments (electric dipoles and quadrupoles).

The hard-body idealization of the interactions is very convenient in that it is easy to parametrize—by simply assigning an effective van der Waals radius to each atom or group of atoms in the molecule—and it is known to convey rather accurately the structural effects of the actual repulsive intermolecular forces as reflected, for example, in the intermolecular correlations in simple liquids. On the other hand, an important limitation of the hard-body picture is that in the absence of additional "soft" forces, it leads to strictly athermal phases and this is in direct contradiction with the sensitivity to temperature variations observed in thermotropic liquid crystals. It is thus clear that a realistic description of mesogen−mesogen interactions will necessarily involve a soft component. However, for those situations where one is mainly concerned with the mechanism of orientation rather than with the detailed effects of temperature on phase stability, it is useful to test if such a simple picture, one wherein ordering can be predicted simply from shape and site-specific interactions (electrostatic moments, hydrogen bonding, ...), can indeed be applied to real mesogens. Thus, the question addressed in this work is: *To what extent can the hard-body picture—molecular shape in the purely geometrical sense—provide a quantitatively accurate description of the mesogen's interaction with a probe solute in the absence of electrostatic or other site-specific interactions?*

In order to obtain an answer of practical utility it is desirable to consider the variation of solute ordering over a wide temperature range, preferably using mesogens and solute molecules without permanent electrostatic moments. However, common liquid crystalline solvents having a reasonably wide nematic range exhibit substantial electrostatic interactions. One is therefore led to the experimental situation wherein one can only choose a class of solutes that are free of appreciable electrostatic moments. In such a class the leading electrostatic interaction involves the polarizability which, as shown in ref 11, has a relatively negligible contribution to solute ordering.

In the present work we have chosen a series of deuterated cycloalkanes as solutes (see Table 1) and the nematic liquid crystal ZLI2452 as the solvent. This class of solutes fits the above requirements rather well: The cycloalkane solutes are for all practical purposes free of electrostatic moments and the solvent (which consists of a mixture of mesogens including cyano- and alkyl-substituted phenylcyclohexanes and biphenylcyclohexanes, alkylcyclohexylbiphenylcyclohexanes, and cyclohexylcarbonates) has a nematic range of 120 °C, one of the widest exhibited by liquid-crystalline solvents. These solute−solvent pairs therefore are potentially a sensitive test system for the evaluation of the adequacy (or inadequacy) of the hard-body interaction mechanism of solute ordering and concomitantly enable us to test the assumption of neglecting the induced electrostatic interactions. A further advantage is that most of the solutes are virtually rigid and thus the analysis is free of the possible ambiguities associated with conformational changes although a similar study[12] in which the solutes were *n*-alkanes showed that the hard-body model combined with the standard rotational isomeric state model for the conformations gives an excellent description of the segmental order parameters of the flexible solute at a given temperature.

The experimental determination of solute orientational ordering is most conveniently done by NMR spectroscopy. Proton NMR studies in liquid crystals initially focused on molecular structure determinations of rigid solutes dissolved in nematic solvents.[13] NMR measurements, aside from providing the order parameters for testing the molecular model, are also interesting in a somewhat different context, namely the study of the dynamics of interconversion between different molecular forms of some of the solutes in two limiting regimes: in the rapid interconversion regime one obtains a conformationally averaged solute structure and, in the slow exchange regime, a superposition of solute spectra reflecting the probabilities of various solute conformers.[14] This is relevant to some of the solutes considered here (cyclohexane,[14] dimethylcyclohexane[15]). Additionally, the NMR spectra of solute probe molecules dissolved in mesophases can be used to delineate properties of liquid-crystalline phases[16] as the probe's orientational order often reflects the ordering of mesogens. In the case of the deuterium nucleus, the incompletely averaged NMR interactions are dominated by the quadrupolar coupling, giving simple spectra that make deuterated solutes particularly useful in this respect. Such probes have been extensively used to study mesophase symmetries, to map out textures (the director field distribution), and to infer the nature of mesogen ordering in various phases.

While symmetry and texture characteristics are generally well reflected in the NMR spectra of probe molecules,[17] the ordering properties of the mesogen are faithfully reflected only when the solute and solvent molecules are sufficiently similar in shape and electronic structure. Specific affinities—electrostatic interactions, hydrogen bonding, etc.—in conjunction with size and shape considerations may strongly affect the ordering of the solutes, even to the extent that the temperature dependence of solute ordering can be opposite to that of the solvent itself.[18] While specific affinities limit a solute's utility as a probe of mesophase behavior, the related effects provide an opportunity to study the mechanisms through which ordering is transmitted

(12) Vanakaras, A. G.; Photinos, D. J. *Mol. Cryst. Liq. Cryst.* **1995**, *262*, 463.
(13) Meiboom, S.; Snyder, L. C. *Science* **1968**, *162*, 1337.
(14) Poupko, R.; Luz, Z. *J. Chem. Phys.* **1981**, *75*, 1675.
(15) Müller, K.; Luz, Z.; Poupko, R.; Zimmermann, H. *Liq. Cryst.* **1992**, *11*, 547.
(16) Emsley, J. W., Ed. *Nuclear Magnetic Resonance of Liquid Crystals;* Reidel: Dordrecht, 1985.
(17) Luz, Z.; Meiboom, S. *J. Chem. Phys.* **1973**, *59*, 275.
(18) Goldfarb, D.; Luz, Z.; Zimmermann, H. *J. Phys.* **1982**, *43*, 421, 1255.

from the solvent to the solute molecules. However, to obtain such fundamental information from solute order parameter data, one needs a molecular theory that explicitly relates the orientational order to the underlying interactions. Conversely, NMR results may be used to test molecular theories.

In section II we briefly summarize the theory advanced by Terzis and Photinos[11] with emphasis on the purely hard-body component of the interaction. After a short Experimental Section summarizing the deuteration procedures, the NMR measurements and the molecular mechanics calculations, we present the experimental results for the order parameters (section IV). These include compounds measured in the present work, as well as results obtained earlier. In section V the calculation procedure is described and the results of the calculations are compared with experiments. The significance of the results is discussed and the conclusions are delineated in section VI.

II. Theoretical Background

The orientational order of a rigid probe molecule in a uniaxial nematic solvent may be described in terms of the five elements of the symmetric-traceless ordering matrix,[19,20]

$$S_{ab} = \int f(\omega)\frac{1}{2}(3\cos\theta_a \cos\theta_b - \delta_{ab})\, d\omega \qquad \text{(II.1)}$$

where θ_a ($a = x', y', z'$)is the angle between the a-axis fixed in the molecular frame and the director and $f(\omega)$ is the orientational distribution function of the solute, with the angle ω ($=\theta,\phi$) corresponding to the orientation of the director in the molecular frame ($\theta = \theta_{z'}$, $\sin\theta\cos\phi = \cos\theta_{x'}$, $\sin\theta\sin\phi = \cos\theta_{y'}$). Thus if $f(\omega)$ is known, the components of S_{ab} can be calculated. This distribution function is conveniently expressed in terms of the potential of mean torque, $V(\omega)$,

$$f(\omega) = \frac{1}{Z}\exp[-V(\omega)/kT] \qquad \text{(II.2)}$$

where Z is a normalization constant. In the theory of Terzis and Photinos (ref 11, to which the reader is directed for details) $V(\omega)$ is expressed in terms of a specific charge distribution, van der Waals interactions, and shape factors of the solute and solvent molecules. The solutions are assumed to be dilute so that solute−solute interactions can be neglected. When only hard-body interactions are considered, the interaction between a pair of solvent−solute molecules is completely described by means of the solute's shape function, $g^{H}(\Omega,\mathbf{r})$, where $\mathbf{r}$ and Ω are respectively the position vector and orientation of the solvent molecule relative to the solute. This function vanishes if the volumes of two molecules intersect and is otherwise equal to one. The potential of mean torque $V(\omega)$ experienced by a solute molecule is then proportional to the orientational average of its excluded volume with respect to the solvent molecules,

$$\frac{V(\omega)}{kT} = \frac{N}{V}\int d\mathbf{r}\, d\omega'\, \tilde{f}(\omega')[1 - g^{H}(\Omega,\mathbf{r})] \qquad \text{(II.3)}$$

where N/V is the number density of the solvent molecules and $\tilde{f}(\omega')$ is their orientational distribution function, with ω' ($=\theta',\phi'$) denoting the orientation of the solvent molecule relative to the director.

To evaluate the potential of mean torque from (II.3) one first integrates over $\mathbf{r}$ to obtain the excluded volume function,

$$C(\Omega) = \frac{1}{\upsilon}\int d\mathbf{r}\,[1 - g^{H}(\Omega,\mathbf{r})] \qquad \text{(II.4)}$$

where υ is the volume of a mesogen molecule. To simplify the calculations it is usually assumed that the mesogens are axially symmetric objects (spherocylinders, in the present calculations). In this case $C(\Omega)$ is a function of only the polar and azimuthal angles, Θ and Φ, of the symmetry axis of the solvent molecule relative the solute frame and consequently it can be expanded in spherical harmonics

$$C(\Theta,\Phi) = \sum_{l,m} C_{l,m} Y^{l}_{m}(\Theta,\Phi) \qquad \text{(II.5)}$$

For a given solvent−solute pair the shape function is determined from eq II.4 and then the expansion coefficients are obtained according to the series inversion relation

$$C_{l,m} = \int d\cos\Theta\, d\Phi C(\Theta,\Phi) Y^{l}_{m}(\Theta,\Phi)^{*} \qquad \text{(II.6)}$$

To perform the averaging of (II.3) over the solvent orientations $\tilde{f}(\omega')$ we first express the excluded volume function in the reference frame of the nematic director using the transformation

$$Y^{l}_{m}(\Theta,\Phi) = \sum_{m'} D^{l}_{m,m'}(\phi,\theta,\psi)^{*} Y^{l}_{m'}(\theta',\phi') \qquad \text{(II.7)}$$

where $D^{l}_{m,m'}$ are the Wigner rotation matrices and ϕ, θ, ψ denote the Euler angles of the solute's molecular frame relative to a frame x_D, y_D, z_D in which the nematic director is along the z_D-axis. Substituting into (II.5) and recalling that for uniaxial solvent molecules $f(\omega')$ is independent of ϕ' finally yields for the potential of mean torque (eq II.3)

$$\frac{V(\theta,\phi)}{kT} = \frac{N\upsilon}{V}\sum_{l,m} C_{l,m}\langle P_l\rangle Y^{l}_{m}(\theta,\phi) \qquad \text{(II.8)}$$

where we have used the identity $D^{l}_{m,0}(\phi,\theta,\psi)^{*} = (4\pi/(2l+1))^{1/2} Y^{l}_{m}(\theta,\phi)$ and the customary definition of the solvent order parameters $\langle P_l\rangle$

$$\langle P_l\rangle = \sqrt{\frac{4\pi}{2l+1}}\int \tilde{f}(\omega') Y^{l}_{0}(\omega')\, d\omega' \qquad \text{(II.9)}$$

These order parameters have non-vanishing values only for even rank l.

III. Experimental Section

A. Materials. Perdeuterated cyclohexane and methylcyclohexane were purchased from Aldrich, while perdeuterated *trans*-decalin was obtained from Cambridge Isotopes. The nematic mixture, ZLI2452, was obtained from Merck. The solute concentrations in the various solutions are given in Table 1. The experimental results for compounds **III**, **IV**, and **VII** are from ref 15 and ref 21; 1,4-*trans*-dimethylcyclohexane (compound **V**) was prepared as described in ref 15 and also for the *cis* isomer. The two isomers have similar boiling points and are therefore difficult to separate by fractional distillation. In these experiments we used the first distillation fraction for recording the spectrum of the *trans* isomer. This fraction contained 30% of the *cis* isomer, but as explained below their signals could readily be distinguished by their different dynamic behavior.

B. NMR Measurements. The deuterium NMR measurements were performed at 46.07 MHz on a Bruker CXP300 spectrometer, using the quadrupole echo pulse sequence. The details are as described in ref 15.

(19) Saupe, A. *Z. Naturforsch.* **1964**, *19a*, 161.
(20) Snyder, L. C. *J. Chem. Phys.* **1965**, *43*, 4041.
(21) Boeffel, C.; Luz, Z.; Poupko, R.; Zimmermann, H. *J. Am. Chem. Soc.* **1990**, *112*, 7158.

Table 2. Atomic Coordinates for the Carbon and Hydrogen Atoms in Compounds **II**, **IV**, and **VI** in the Coordinate Systems Shown in Figure 1

	x'/Å	y'/Å	z'/Å
Methylcyclohexane (**II**)			
C_1	+0.714	−1.297	+0.000
$C_{2,6}$	+0.001	−0.771	±1.262
$C_{3,5}$	+0.000	+0.772	±1.261
C_4	−0.715	+1.297	−0.002
D^a_1(eq conf)	+1.722	−0.858	+0.001
D^e_1(ax conf)	+0.689	−2.386	+0.000
$D^a_{2,6}$	−1.040	−1.125	±1.268
$D^e_{2,6}$	+0.498	−1.121	±2.147
$D^a_{3,5}$	+1.040	+1.125	±1.268
$D^e_{3,5}$	−0.498	+1.121	±2.146
D^a_4	−1.722	+0.858	−0.001
D^e_4	−0.689	+2.386	+0.000
Me(eq conf)	−0.678	−2.839	−0.001
Me(ax conf)	+2.175	−0.801	+0.001
1,4-*trans*-Dimethylcyclohexane (**V**)			
C_1	+0.690	−1.321	+0.000
C_2	+0.000	−0.768	+1.259
D^a_1	+1.750	−0.979	+0.000
D^a_2	−1.046	−1.140	+1.304
D^e_2	+0.518	−1.138	+2.169
Me[1]	+0.686	−2.858	+0.000
trans-Decalin (**VI**)			
C_1	+0.687	−1.308	+1.269
C_2	+0.000	−0.769	+2.533
C_9	+0.001	−0.771	+0.000
D^a_1	+1.756	−1.007	+1.273
D^e_1	+0.658	−2.419	+1.276
D^a_2	−1.046	−1.142	+2.577
D^e_2	+0.521	−1.148	+3.439
D^a_9	−1.054	−1.126	+0.000

C. Molecular Geometry. Accurate geometries of the solute molecules are essential for both the analysis of the experimental spectra in terms of orientational order parameters and their calculation according to the theory in section II. Since no crystallographic data are available for the probe molecules we used geometries obtained from molecular mechanics calculations, using MM2(85)[22] or AM1[23] force field parameters, except that for cyclohexane, an idealized diamond structure was used. The atomic coordinates for compounds **II**, **V**, and **VI** are summarized in Table 2. Those for compounds **III**, **IV**, and **VII** are given in earlier publications.[15,21] Note that we have re-labeled the atomic positions and redefined the coordinate axes, so that $z = z'$ is always a unique-symmetry axis, and the coordinate system is right-handed with the angles α (see below) always positive (see Figure 1).

IV. Deuterium NMR Spectra and the Experimental Orientation Order Parameters

Examples of spectra for cyclohexane (**I**), methylcyclohexane (**II**), 1,4-*trans*-dimethylcyclohexane (**V**), and *trans*-decalin (**VI**), dissolved in ZLI2452, are shown in Figure 2. They consist of superpositions of doublets according to the number of equivalent or nearly equivalent groups of deuterons in the molecule. Also shown in the figure are the peak assignments for the various deuterons. These could usually be determined on the basis of their relative intensities and geometrical considerations. When complete identification could not be made by such considerations the assignment was obtained from the fitting procedure described below. Likewise, although the relative signs of the quadrupole interaction constants could often be guessed, they were definitely determined only by the fitting procedure.

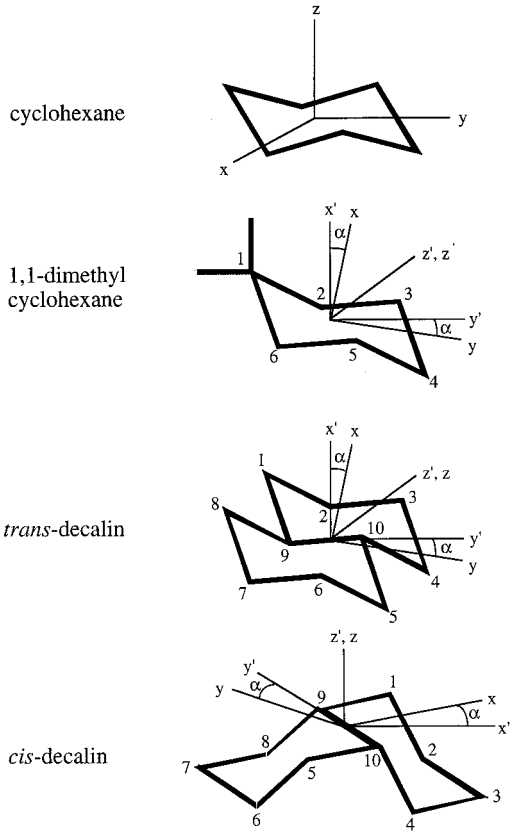

Figure 1. Coordinate systems used for the compounds studied. (a) Cyclohexane (D_{3d} symmetry): z is parallel to the C_3 axis with the origin at the inversion center. (b) Substituted cyclohexanes (compounds **II** to **V**, C_s and C_{2h} symmetries): z is perpendicular to the symmetry plane with origin at the intersection point of the diagonals joining carbons 2−5 and 3−6, y' is along the intersection line between the symmetry plane and the plane containing atoms 2, 3, 5, and 6. (c) *trans*-Decalin (C_{2h} symmetry): z is perpendicular to the symmetry plane with origin at the midpoint of the C_9-C_{10} bond, y' is along the C_9-C_{10} bond. (d) *cis*-Decalin (C_2 symmetry): z is parallel to the C_2 axis with origin at the midpoint of the C_9-C_{10} bond, y' is along the C_9-C_{10} bond. In all cases x', y', and z form a right handed system. The x, y, z coordinates represent the principal axes of the ordering matrix.

The spectrum of cyclohexane has been studied in other liquid crystalline solvents.[14] At around room temperature it exhibits dynamic effects due to ring inversion. The two spectra shown in Figure 2 are for 2.3% cyclohexane in ZLI2452 solutions and correspond to the slow and fast interconversion limits respectively. In the low-temperature spectrum (−40 °C) the two doublets are due to the axial (a) and equatorial deuterons (e), while at high temperature (85 °C) only a single coalesced doublet (a/e) is observed. The spectra were interpreted as in ref 14.

The various peaks in the spectrum of methylcyclohexane can readily be assigned to the (weakly resolved) equatorial 4e, the axial, the other equatorial, and the methyl deuterons, on the basis of their relative intensities, 1:6:4:3 (see the third spectrum in Figure 2). The six axial deuterons are not strictly equivalent, but they become nearly so due to the fact that all the axial C−D bonds are nearly parallel. The peaks due to these deuterons do indeed split at higher temperatures. Likewise the four equatorial deuterons divide into two groups having similar quadrupole interactions; they remain degenerate, however, at higher temperatures.

(22) Allinger, N. L. *J. Am. Chem. Soc.* **1977**, *99*, 8129. Burkert, U.; Allinger, N. L. *Molecular Mechanics;* American Chemical Society: Washington, DC, 1982.

(23) We use the AM1 semiempirical molecular orbital method. It is a method included in the Mopac package of the Sybyl Molecular Mechanics software. Hehre, W. J.; Radom, L.; Shleyer, P. V. R.; Pople, J. *Ab Initio Molecular Orbital Theory;* Wiley: New York, 1986. Stewart, J. J. *J. Comp.-Aided Mol. Design* **1990**, *4*, no. 1.

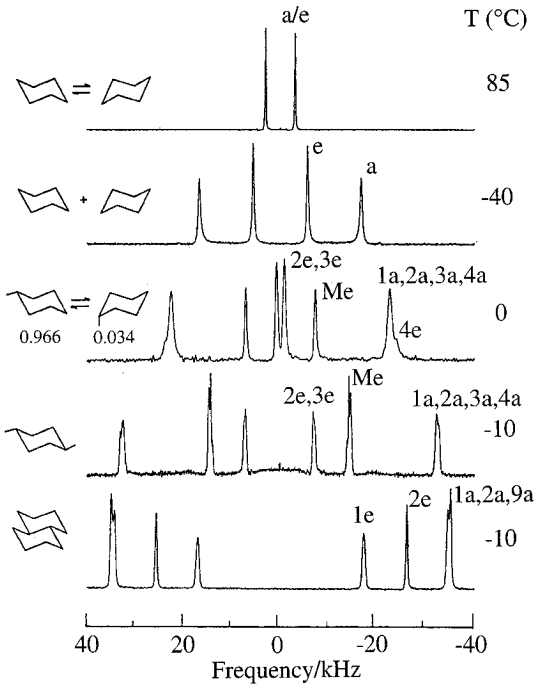

Figure 2. Deuterium NMR spectra and peak assignment (one of each group of equivalent deuterons) of deuterated solutes dissolved in the nematic solvent, ZLI2452. From top to bottom: cyclohexane at 85 and −40 °C; methylcyclohexane at 0 °C; 1,4-*trans*-dimethylcyclohexane at −10 °C (the background signal is due to the dynamic spectrum of the *cis* isomer, see Experimental Section); *trans*-decalin at −10 °C.

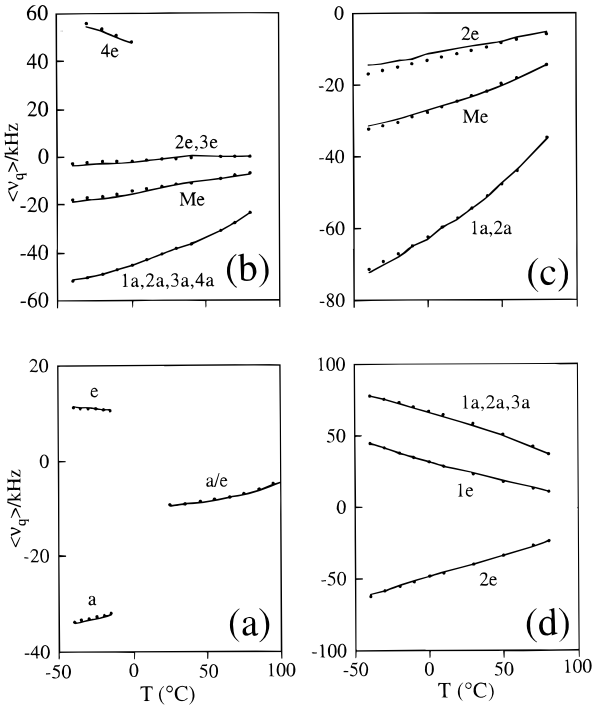

Figure 3. Quadrupole splittings in ZLI2452 solutions of the following deuterated compounds: (a) cyclohexane, (b) methylcyclohexane, (c) 1,4-*trans*-dimethylcyclohexane, and (d) *trans*-decalin. The points are experimental, while the curves are calculated from the theoretically derived order parameters. The peak assignment is as in Figure 2, with the signs determined as explained in the text.

The sample of 1,4-*trans*-dimethylcyclohexane contained a significant amount (30%) of the *cis* isomer (compound **IV**). However, since the latter undergoes dynamic line broadening due to ring inversion[15] (see the broad central background signal in the fourth spectrum of Figure 2), the spectra of the two isomers could be readily distinguished. The deuterons in the *trans* isomer divide into three groups, methyl, axial, and equatorial, whose signals could readily be assigned on the basis of their relative intensities, 3:6:4. As for the case of methylcyclohexane, the axial deuterons are only approximately equivalent. This accounts for the small splitting observed in the corresponding doublet. The splitting of the methyl doublet is due to dipolar interactions between the methyl deuterons.

Due to the high symmetry of *trans*-decalin, its eighteen deuterons divide into five groups. However, all the axial deuterons turn out to have very similar quadrupole splittings and give rise to the intense, weakly split outer doublet (lower spectrum in Figure 2). The other two peaks, due to the groups of equatorial deuterons 2,3,5,6 and 1,4,5,8, were identified by the quantitative analysis of the spectrum.

Plots of the quadrupole splittings, $\langle\nu_q{}^i\rangle$ (half of the doublet separation), as a function of temperature for the various deuterons in compounds **I**, **II**, **V**, and **VI** are shown in Figure 3, where the signs were determined by the analysis, as described below.

The various order parameters were obtained by fitting the experimental $\langle\nu_q{}^i\rangle$'s to the equation,[19]

$$\langle\nu_q{}^i\rangle = \nu_q{}^i \sum_{ab} S_{ab} \cos\theta_a{}^i \cos\theta_b{}^i \qquad \text{(IV.1)}$$

where $\theta_a{}^i$ is the angle between the C−D^i bond and the *a*-axis and $\nu_q{}^i$ is the static quadrupole interaction constant for the *i*th deuteron, assumed to be axially symmetric with the unique axis parallel to the C−D bond ($\nu_q{}^a = 126$ kHz for all aliphatic deuterons, except that for the methyl deuterons $\nu_q{}^m = -\nu_q{}^a/3 = -42$ kHz). The analysis of the S_{ab}'s can be significantly simplified for solute molecules having special symmetries. In such cases not all order parameters are independent and by choosing appropriate coordinate systems in the molecular frame, their number can be reduced. For molecules with a 3-fold symmetry axis, taking $z = z'$ parallel to the C_3-axis renders S_{zz} the only independent order parameter. Accordingly, for cyclohexane, recalling that $S_{x'x'} + S_{y'y'} + S_{z'z'} = 0$, eq IV.1 reduces to

$$\langle\nu_q{}^i\rangle = \nu_q{}^i S_{zz} \frac{1}{2}(3\cos^2\theta_z{}^i - 1) \qquad \text{(IV.2)}$$

with only one orientational order parameter, which can straightforwardly be obtained from the experimental data.

For molecules having C_s, C_{2h}, or C_2 symmetries, as is the case for the rest of the compounds in Table 1, taking *z* along the C_2-axis or perpendicular to the symmetry plane leads to S_{zz}, $S_{x'x'} - S_{y'y'}$, and $S_{x'y'}$ as the only non-zero parameters. In this case, using the coordinate systems of Figure 1, eq IV.1 becomes,

$$\langle\nu_q{}^i\rangle = \nu_q{}^i(S_{x'x'}\cos^2\theta_{x'}{}^i + S_{y'y'}\cos^2\theta_{y'}{}^i + S_{zz}\cos^2\theta_z{}^i + 2S_{x'y'}\cos\theta_{x'}{}^i\cos\theta_{y'}{}^i) \qquad \text{(IV.3)}$$

Thus there are three order parameters to be determined (e.g., S_{zz}, $S_{x'x'} - S_{y'y'}$, and $S_{x'y'}$), while the number of $\langle\nu_q{}^i\rangle$'s is considerably larger. By optimized fitting to the experimental results it is therefore possible to confirm the peak assignment, determine the relative sign of the quadrupole splittings, and derive the S_{ab}'s.

We find it more convenient to express the results in the principal coordinate system of the ordering matrix. This system *x*, *y*, *z* is related to the original *x*′, *y*′, *z*′ one through a rotation by an angle α about *z*′, where

$$\mathrm{tg}(2\alpha) = \frac{2S_{x'y'}}{S_{x'x'} - S_{y'y'}} \qquad \text{(IV.4)}$$

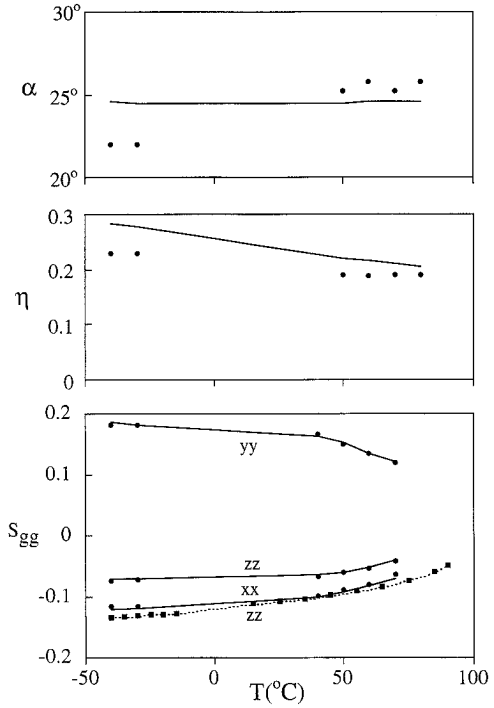

Figure 4. Plots of the molecular orientational order parameters, the asymmetry parameter, and the angle α between *x* and *x*′ for the cyclohexane and 1,1-dimethylcyclohexane. The points are experimental results from the NMR measurements (circles for 1,1-dimethylcyclohexane and squares for cyclohexane), while the lines (solid for 1,1-dimethylcyclohexane and dashed for cyclohexane) are calculated as explained in the text.

In this coordinate system the order parameters become,

$$S_{zz} = S_{z'z'}$$

$$S_{xx} = S_{x'x'}\cos^2\alpha + S_{y'y'}\sin^2\alpha + S_{x'y'}\sin(2\alpha) \quad \text{(IV.5)}$$

$$S_{yy} = S_{x'x'}\sin^2\alpha + S_{y'y'}\cos^2\alpha - S_{x'y'}\sin(2\alpha)$$

The points in Figures 4−7 represent the order parameters in this principal coordinate frame, and the angle α is as defined above. In this frame the $\langle \nu_q^i \rangle$'s can be written as

$$\langle \nu_q^i \rangle = \nu_q^i S_{cc}\left[\frac{1}{2}(3\cos^2\theta_c^i - 1) + \frac{1}{2}\eta(\cos^2\theta_a^i - \cos^2\theta_b^i)\right] \quad \text{(IV.6)}$$

where

$$\eta = \frac{S_{aa} - S_{bb}}{S_{cc}} \quad \text{(IV.7)}$$

and we have chosen $|S_{cc}| > |S_{bb}| > |S_{aa}|$, leading to $\eta > 0$. In all compounds (**II** to **VII**) having $\eta \neq 0$, the *c*-axis corresponded to the longest dimension of the molecule. We therefore set the sign of S_{cc} positive in order to conform with the expectation that the molecules prefer to align with their long axis parallel to the director. This assignment was used to fix the signs of the $\langle \nu_q^i \rangle$'s and of the S_{aa}'s in Figures 3−7.

The experimental results in Figures 4, 6, and 7 for compounds **I** and **V** were determined from the measured splittings of Figure 3 whereas the results for compounds **III**, **IV**, and **VII** are taken from ref 15 and ref 21. Note the absence of numerical data at intermediate temperatures for compounds **III** and **IV** and at high temperatures for compound **VII**, where dynamic line-broadening prevented direct experimental determination of the order parameters.

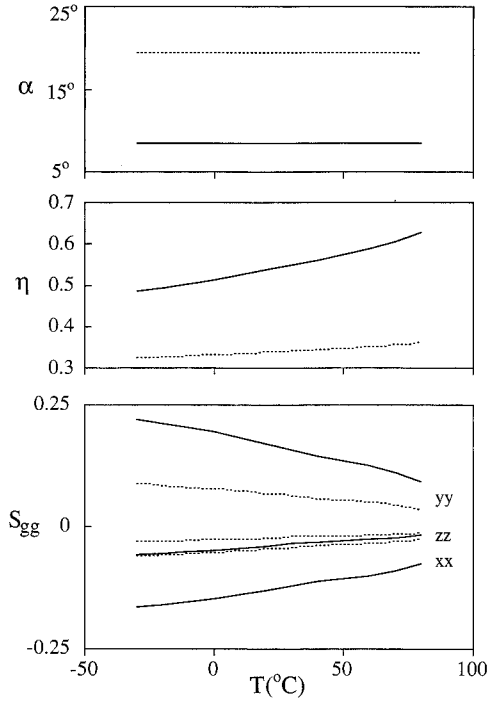

Figure 5. Plots of the molecular orientational order parameters, the asymmetry parameter, and the angle α between *x* and *x*′ for the methylcyclohexane (equatorial and axial). The lines (solid for equatorial and dashed for axial) are calculated results as explained in the text.

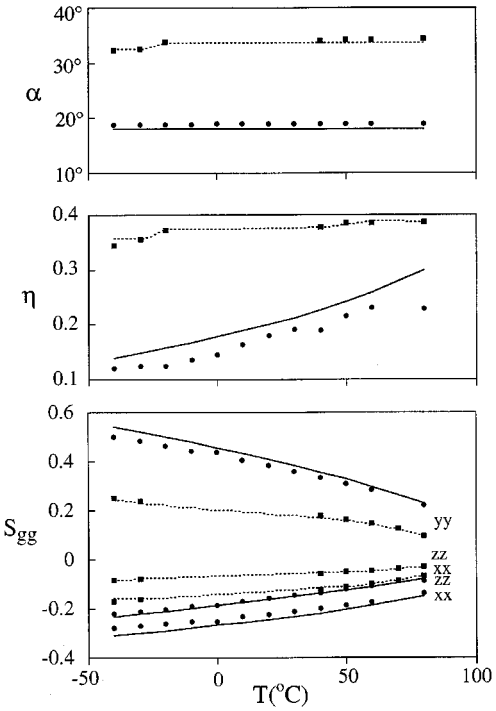

Figure 6. Plots of the molecular orientational order parameters, the asymmetry parameter, and the angle α between *x* and *x*′ for the 1,4-*trans*-dimethylcyclohexane and 1,4-*cis*-dimethylcyclohexane. The points are experimental results from the NMR measurements (circles for *trans* and squares for *cis*), while the lines (solid for *trans* and dashed for *cis*) are calculated as explained in the text.

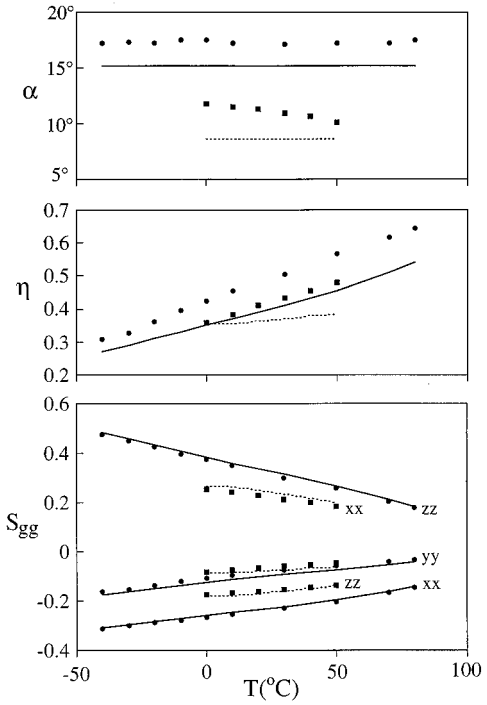

Figure 7. Plots of the molecular orientational order parameters, the asymmetry parameter, and the angle α between *x* and *x*′ for the 1,4-*trans*-decalin and 1,4-*cis*-decalin. The points are experimental results from the NMR measurements (circles for *trans* and squares for *cis*), while the lines (solid for *trans* and dashed for *cis*) are calculated as explained in the text.

V. Hard-Body Model Calculations of Solute Order Parameters

In applying the theory of section II to the calculation of $V(\omega)/kT$, we limited the summation in eq II.8 to the $l = 2$ terms. The $l = 0$ term is independent of orientation and corresponds to the average excluded volume of the solvent−solute system. It has therefore no effect on the solute ordering. The $C_{2,m}$ terms were found to be sufficient to bring out the different ordering characteristics of the various solutes and to provide good estimates of the experimental order parameters. Higher rank terms turned out to have rather limited effects on the final results, and were omitted for simplicity. Equation II.8 thus becomes,

$$\frac{V(\theta,\phi)}{kT} = p\sum_m C_{2,m}Y^2{}_m(\theta,\phi) \qquad \text{(V.1)}$$

where

$$p = \frac{N\nu}{V}\langle P_2\rangle \qquad \text{(V.2)}$$

Since the potential in eq V.1 is real we prefer to write it in terms of real spherical harmonics and real coefficients,

$$\frac{V(\theta,\phi)}{kT} = 5p\Big[C_{z^2}\frac{1}{2}(3\cos^2\theta - 1) + C_{xz}\sin2\theta\cos\phi + C_{yz}\sin2\theta\sin\phi + C_{x^2-y^2}\frac{1}{2}\sin^2\theta\cos2\phi + C_{xy}\sin^2\theta\sin2\phi\Big] \qquad \text{(V.3)}$$

where

$$C_{z^2} = \sqrt{\frac{1}{20\pi}}C_{2,0}, \quad C_{xz} = -\sqrt{\frac{3}{40\pi}}\mathrm{Re}\{C_{2,1}\},$$
$$C_{yz} = -\sqrt{\frac{3}{40\pi}}\mathrm{Im}\{C_{2,1}\}, \quad C_{x^2-y^2} = \sqrt{\frac{6}{5\pi}}\mathrm{Re}\{C_{2,2}\},$$
$$C_{xy} = \sqrt{\frac{3}{160\pi}}\mathrm{Im}\{C_{2,2}\} \qquad \text{(V.4)}$$

As in the case of the ordering matrix S_{ab}, symmetry considerations can reduce the number of non-zero C_{ab} coefficients. Thus for cyclohexane, taking *z* parallel to the C_3-axis, leads to C_{z^2} as the only non-zero coefficient, while for all other compounds of Table 1, taking *z* parallel to the C_2-axis or perpendicular to the reflection plane results in $C_{xz} = C_{yz} = 0$.

The excluded volume functions, $C(\Theta,\Phi)$, for the various solutes were calculated by considering a solvent molecule oriented at Θ,Φ, with respect to the solute coordinate system and integrating over the whole **r** space. The solvent molecules were assumed to be spherocylinders with length $L + D$ and diameter D. The effective length of the solvent molecules was determined by the optimization procedure described below. The diameter was set at $D = 5.2$ Å which is a typical value for calamitic liquid crystals consisting of molecules with benzene moieties along their long axis. The solute shape was constructed from spheres positioned at the coordinates of the carbon atoms with a van der Waals radius, $R_{vdw} = 1.77$ Å, and it accounts also for the hydrogens bound to the carbon "united atoms".[24]

Once the shape functions for the various solutes were determined the expansion coefficients $C_{l,m}$ were calculated by numerical integration of eqs II.4 and II.6 for a particular L/D. Next the parameter p (eq V.2) needed to be fixed. Ideally this parameter should be identical for all solutes at the same temperature. We therefore initially chose one particular temperature for which experimental data for most compounds were available (−40 °C) and varied p to minimize the overall sum of the squares of the deviations of the calculated order parameters from the experimental values, namely $\sum_{i,\alpha,\beta}[S_{\alpha\beta}{}^i(\mathrm{cal}) - S_{\alpha\beta}{}^i(\mathrm{exp})]^2$, where the superscript i refers to the solute. The procedure was then repeated for different L/D values, each time optimizing the p parameter at −40 °C, until an overall best fit was obtained for all the results at that temperature. This analysis gave the best fit values $L/D = 3.31$, corresponding to $\upsilon = 439$ Å^3, for the solvent and the C_{ab}'s listed in Table 3 for the various solutes. To extend the fitting over the entire temperature range we kept the values of L/D and of the C_{ab}'s fixed at the above quoted values and optimized the parameter p at each temperature. At this stage we relaxed the requirement that p be the same for all solutes. In the final calculations the differences in the optimal values of p were indeed small (see below). For the evaluation of the solute order parameters from the experimental data we diagonalized, where appropriate, the ordering matrix using eqs IV.4 and IV.5 and finally calculated η using eq IV.7.

In several instances the expansion in eq V.1 was extended to include the leading $l = 4$ term, $C_{4,0}$,

$$\frac{N\nu}{V}\langle P_4\rangle C_{4,0}Y_0^4 = \frac{N\nu}{V}\langle P_4\rangle C_{z^4}\frac{1}{8}(3 - 30\cos^2\theta + 35\cos^4\theta) \qquad \text{(V.5)}$$

where $C_{z^4} = (3/4\pi)^{1/2}C_{4,0}$ (see Table 3 for the numerical values of C_{z^4}). However, the contribution of this term to the calculated S_{ab}'s was found to be marginal. For this reason and also in view of the other more drastic simplifications employed in the

(24) Bondi, A. *J. Phys. Chem.* **1964**, *68*, 441.
(25) Aliev, A. E.; Harris, K. D. M. *J. Am. Chem. Soc.* **1993**, *115*, 6363.

Table 3. Expansion Coefficients of the Excluded Volume Function (Eqs II.6 and V.4) for Each of the Solutes Studied[a]

compd no.	name	$C_{0,0}$	C_{z^2}	$C_{x^2-y^2}$	C_{xy}	C_{z^4}
I	cyclohexane	17.895	+0.129	0.000	0.000	-0.023
II(a)	methylcyclohexane (axial)	19.220	-0.015	+0.143	+0.045	+0.018
II(e)	methylcyclohexane (equatorial)	19.577	-0.013	+0.329	+0.060	+0.010
III	1,1-dimethylcyclohexane	20.667	+0.036	+0.634	+0.200	+0.009
IV	1,4-*cis*-dimethylcyclohexane	20.542	+0.014	+0.361	+0.337	+0.012
V	1,4-*trans*-dimethylcyclohexane	20.884	+0.123	+0.334	+0.155	+0.031
VI	*trans*-decalin	22.539	-0.311	+0.273	+0.062	-0.101
VII	*cis*-decalin	22.230	+0.195	-0.391	-0.061	+0.082

[a] The solvent molecules are represented by spherocylinders of dimensions $L = 17.2$ Å, $D = 5.2$ Å.

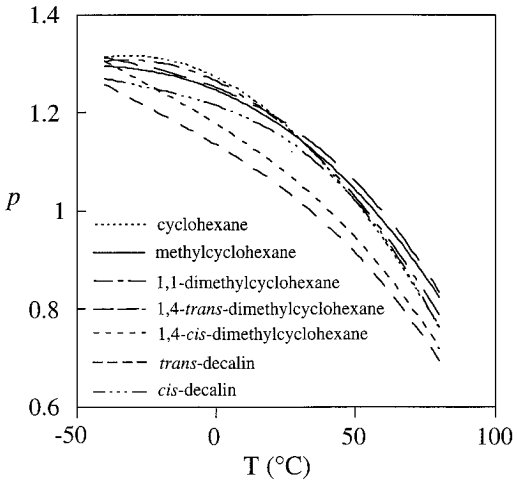

Figure 8. Plots of the temperature dependence of the optimal values of the solvent parameter p as determined from the fits to the measured order parameters of the respective solutes.

modeling, these terms were completely ignored in the final optimization.

In the plots of Figures 3, 4, 6, and 7 the results of the calculations are compared with the results obtained from measurement. The respective optimal values of the parameter p are plotted in Figure 8 where it can be seen that curves pertaining to the different solutes are within a 10% range of a common curve. Before discussing the general implications of these results in the next section, the following specific comments are in order:

The perfect fit of the cyclohexane data is to be expected: There is just one observable (the ratio between the axial and equatorial splittings is determined by the molecular geometry[14]) that can readily be fitted by varying the single adjustable parameter, p. The important feature in this case is that the optimal values of p turned out to be practically identical to the values obtained for the other solutes. Furthermore, the prediction that S_{zz} is negative, although not directly testable from the experimental spectra, is intuitively plausible as it implies that in the absence of other effects, the cyclohexane molecule preferentially orients with its plane parallel to the prolate calamitic solvent molecules.

Attempts to fit the spectra of methylcyclohexane by allowing only for the dominant equatorial isomer gave poor results. This solute exists as a mixture of rapidly (on the NMR time scale) interconverting axial and equatorial isomers. The equilibrium ratio between the two isomers, $P_{\text{axial}}/P_{\text{equatorial}} = \exp(-\Delta G/RT)$, is characterized by a free energy difference of $\Delta G = 7.6$ kJ/mol.[25] At room temperature this yields about 5% for population of the axial conformer. When both isomers are included in the analysis, excellent agreement of the calculated weight-averaged quadrupole splittings with the experimental results is obtained as shown in Figure 3b. The corresponding calculated order parameters are plotted in Figure 5 but without experimental points as these could not be determined separately for the two isomers from the measured splittings.

The agreement between the theoretical and experimental values of the various order parameters is in general quite satisfactory. It might appear that for some solutes there are appreciable deviations in the plots of the parameters η and α (see Figures 6 and 7). It should, however, be kept in mind that both parameters are very sensitive to variations of the numerical values of the order parameters, particularly when these values are small. Thus, toward the high-temperature end of the plots, the estimated errors in the experimental values are as high as $\pm 10\%$ for η and $\pm 3°$ for α. This, combining the relatively broad range of variation of both η (0.1 to 0.7) and α (5° to 35°) indicates that the overall accordance of the results for all seven solutes is in fact impressive.

Finally, to get some qualitative insight into the relation between the orientational ordering and the shape anisotropy of these solutes it is useful to relate the components of the ordering tensor S_{ab} with those of the 2nd rank excluded volume interaction tensor C_{ab}. When higher rank contributions to the potential of mean torque are neglected as is done in eq V.3, these two tensors share a common principal axis frame. Furthermore, in the limit of weak ordering, S_{ab} is proportional to C_{ab}, as may readily be seen from eqs V.3, II.1, and II.2 on ignoring quadratic or higher terms in the Taylor expansion of $f(\omega)$ in powers of p.

VI. Discussion and Conclusions

The description of cycloalkane solute ordering in terms of purely hard-body interactions with the nematic solvent molecules is essentially in complete agreement with the results of experimental observations as summarized in Figures 3, 4, 6, and 7. This agreement is obtained by optimizing with respect to the parameter p. Since this parameter is a composite property of the nematic solvent it follows that if all the assumptions made in the calculations were perfectly valid, its optimal values should be strictly identical for all the solutes at a given temperature of the solvent, and furthermore, these values should not exceed unity (since p is the product of the packing fraction with the order parameter $\langle P_2 \rangle$, neither of which can become larger than 1). As can be seen from the plots of Figure 8, there are deviations in both respects from this ideal behavior; the deviations from a unique $p(T)$ curve are relatively limited—on the order of 10%—whereas p considerably exceeds the upper bound of unity for all of the solutes at low temperatures. These deviations are the combined result of a number of factors, one of which is the use of a strictly hard-body potential. The other factors can be classified in two categories:

a. Simplifications Made for Computational Expediency. These include (**a.1**) the assignment of a fixed (with temperature and solute type) spherocylindrical shape to the solvent molecules in spite of the fact that the actual solvent is a multicomponent mixture of molecules each exhibiting considerable flexibility and structural complexity (this appears to constitute the major

oversimplification); (**a.2**) the complete neglect of solute−solute interactions, although the solute molecule concentrations are not negligible; and (**a.3**) the neglect of $l > 2$ contributions to the excluded volume interactions. The rectification of (**a.2**) and (**a.3**) is not particularly demanding computationally but it appears to be pointless without the simultaneous rectification of (**a.1**) which, however, would render the computations rather lengthy and complex.

b. Approximations in the Statistical Mechanical Treatment. The calculations are based on the neglect of correlations among the solvent molecules. In other words, a solute molecule interacts fully with all of the solvent molecules but the latter are assumed to interact among themselves indirectly, through the solvent mean field. The inclusion of solvent−solvent correlations complicates considerably the calculations even in the case of spherocylinders, and moreover it is certainly not warranted for quantitative comparisons unless the molecular features of the solvent stated in (**a.1**) are taken into account more realistically.

In view of the above it is hardly surprising that the optimal values of p deviate from the ideal behavior. On the other hand, it is rather encouraging that these deviations show a rather moderate dependence on solute size, to the point that one may fairly accurately determine the order parameters of the solutes of this category given the value of one order parameter for one of the solutes (which is required to specify the appropriate value of p). Lastly, with or without the computational simplifications in (**a**), what appears to be the final compromise underlying the use of the very simple hard-body molecular picture and the neglect of solvent−solvent correlations is the necessity to use a renormalized value for the quantity p. This is analogous to the use of (temperature and density dependent) effective hard-sphere diameters in order to compensate for the removal of longer-ranged interactions in simple liquids.[1] The fact that the renormalized value of p can grow larger than the product of the maximum values of the actual measurable quantities that comprise p leads to a picture wherein the effective volume of the solvent molecule *as seen by a solute molecule* is considerably larger than the actual volume (i.e. the volume associated with the packing and the interactions among the solvent molecules). Such an interpretation is in accord with the large effective values of the solvent packing fraction found in similar calculations involving *n*-alkane solutes.[12]

Acknowledgment. This work was supported by the National Science Foundation Grant No. DMR-9412701 and the Israel Science Foundation administered by the Israel Academy of Sciences and Humanities.

JA953095R